Hydrol. Earth Syst. Sci. Discuss., 9, 9391–9423, 2012
www.hydrol-earth-syst-sci-discuss.net/9/9391/2012/
doi:10.5194/hessd-9-9391-2012

Hydrology and Earth System Sciences Discussions

Snow Accumulation-Melting Model (SAMM) for integrated use in regional scale landslide early warning systems

G. Martelloni[1,*], S. Segoni[1], D. Lagomarsino[1], R. Fanti[1], and F. Catani[1]

[1]University of Firenze, Earth Sciences Department, Via La Pira 4, 50121 Firenze, Italy
[*]now at: University of Firenze, Department of Energy Engineering
(CSDC – Center of the Study of Complex System), Via Santa Marta 3, 50139 Firenze, Italy

Received: 26 July 2012 – Accepted: 1 August 2012 – Published: 10 August 2012

Correspondence to: S. Segoni (samuele.segoni@unifi.it)

Published by Copernicus Publications on behalf of the European Geosciences Union.

Abstract

We propose a simple snow accumulation-melting model (SAMM) to be applied at the regional scale in conjunction with landslide warning systems based on empirical rainfall thresholds.

SAMM follows an intermediate approach between physically based models and empirical temperature index models. It is based on two modules modelling the snow accumulation and the snowmelt processes. Each module is composed by two equations: a conservation of mass equation is solved to model snowpack thickness and an empirical equation for the snow density. The model depends on 13 empirical parameters, whose optimal values were defined with an optimization algorithm (simplex flexible) using calibration measures of snowpack thickness.

From an operational point of view, SAMM uses as input data only temperature and rainfall measurements, bringing the additional advantage of a relatively easy implementation. The snow model validation gave satisfactory results; moreover we simulated an operational employment in a regional scale landslide early warning system (EWS) and found that the EWS forecasting effectiveness was substantially improved when used in conjunction with SAMM.

1 Introduction

In Italy landsliding is one of the most widespread natural hazards, responsible for casualties and major economical losses (Guzzetti, 2000), consequently there is a clear need to set up effective landslide warning systems. Physically based conceptual models rely on a number of input parameters characterized by a spatial organization that is difficult to correctly assess in large-scale distributed applications, therefore they are mainly used in operational monitoring and warning systems that work at the slope (Damiano et al., 2012) or catchment scale (Segoni et al., 2009; Baum et al., 2010). Conversely, regional scale landslide early warning systems are usually based on simpler but effective statistical or empirical correlations with rainfall (Keefer et al., 1987; Aleotti, 2004; Cannon et al., 2011; Martelloni et al., 2011; Segoni et al., 2012), which is commonly accepted as the major cause of landslide triggering (Wieczorek, 1996). Such methodology is widely used at regional scale because it allows considering a single parameter (rainfall) to monitor and forecast landslide occurrence (Rosi et al., 2012).

Despite that, in mid-latitude areas a not negligible number of landslides is commonly triggered by the water released after rapid snowmelt (Chleborad, 1997; Cardinali et al., 2000; Guzzetti et al., 2003; Kawagoe et al., 2009). This leads to the necessity of incorporating snow accumulation and melting modules into landslide regional scale early warning systems. Unfortunately, the coupling of snowmelt models and landslide hazard assessments is not well established and only a few examples exist (Gokceoglu et al., 2005; Naudet et al., 2008; Kawagoe et al., 2009). However, in other fields of research, snow accumulation/depletion models have been implemented with various practical aims ranging from the estimation of hydrologic runoff (Marks et al., 1999; Zanotti et al., 2004; Garen and Marks, 2005; Li and Wang, 2011) to the study and forecasting of snow avalanches (Brun et al., 1989; Bartelt and Lehning, 2002; Rousselot et al., 2010; Takeuchi et al., 2011), the related soil erosion (Ceaglio et al., 2012), and to global atmospheric circulation and weather forecasts (Martin et al., 1996; Bernier et al., 2011).

Depending on the scopes, the scales and the available data, several snow accumulation/melting models have been proposed, and they can be grouped into two main categories. The most sophisticated are spatially distributed models based on equations of mass and energy balance (Bloschl et al., 1991; Zanotti et al., 2004; Garen and Marks, 2005; Herrero et al., 2009). These models, following a mechanistic approach, account for as many as possible physical and chemical process involved in the building and depletion of the snowpack. Such models are rather complex and require several physical parameters including (but not limited to) topography, precipitation, air temperature, wind speed and direction, humidity, downwelling shortwave and longwave radiation, cloud cover, surface pressure. The determination of the exact values of these parameters, and their variation in space and time, is only possible for very

HESSD
9, 9391–9423, 2012

Snow Accumulation-Melting Model (SAMM)

G. Martelloni et al.

well equipped experimental test sites, therefore simplified approaches as temperature-index methods are also widely used (Kustas et al., 1994; Rango and Martinec, 1995; Hock, 1999, 2003, Jost et al., 2012). These models use air temperature as an index to perform an empirical correlation with snowmelt and require only a few parameters (e.g. precipitation, air temperature, snow covered area). Temperature index methods are more simplistic than the aforementioned physical models, nevertheless they can be used with good results and it has been shown that only little additional improvement in model performance is achieved when adopting an energy balance approach (Hock, 2003).

In this paper an intermediate approach between physically based models and empirical temperature index models is used to develop a simple snow accumulation/melting model (SAMM henceforth), to be integrated into a regional scale early warning system based on statistical rainfall thresholds for the occurrence of landslides.

The main objective of SAMM is not an actual distributed modelling of the snowpack, but the development of a methodology to modify the rainfall measurements used as input data in landslide warning systems so as to take into account snow accumulation and depletion.

The paper first presents an overview of the study area, the landslide warning system, the quantity and quality of available experimental data. Then the snow accumulation/melting model is presented with emphasis on the adopted calibration procedure. The results of the calibration are presented and validated, then the application to the SIGMA landslide warning system (Martelloni et al., 2011) is shown and discussed.

2 Materials and methods

2.1 Case study

Emilia Romagna (22 446 km^2) is an Italian region (Fig. 1), which is highly prone to landsliding. Its hills and mountains (Northern Apennines) are interested by both shallow and deep seated landslides: the first are usually triggered by short and exceptionally intense rainstorms and the latter are influenced by moderate but exceptionally prolonged rainfalls (Martelloni et al., 2011).

To manage the hazard related to both kinds of landslides, the Emilia Romagna Civil Protection Agency uses, among the others, a warning system called SIGMA (*Sistema Integrato Gestione Monitoraggio Allerta*, "Integrated service for managing and monitoring alerts") (Martelloni et al., 2011). The system is based on a series of statistical rainfall thresholds, which are compared with two different periods of cumulative rainfall: daily checks of the 1 day, 2 days and 3 days cumulative rainfall are related to the occurrence of shallow landslides; a series of daily checks over a longer and variable time window (up to 243 days, depending on the seasonality) is related to the activation or reactivation of deep seated landslides in low-permeability terrains. A decisional algorithm combines different thresholds (corresponding to rainstorms with increasing severity) and issues a warning level in accordance with the regional civil protection guidelines. SIGMA combines in the decisional algorithm rainfall forecasts and the hourly rainfall measurements received from an automated regional network. The hilly and mountainous territory of Emilia Romagna is partitioned into 19 Territorial Units (TUs), which have a typical areal extension of a few hundred squared kilometres and can be considered quite homogeneous from a geomorphological and meteorological point of view (Fig. 1).

All TUs have a pluviometric regime characterized by rainy autumns and springs and dry summers, but the average precipitations are very different (Fig. 2). In most part of TUs, snow is an exceptional phenomenon and when it occurs the snowpack is likely to melt in a few days. On the contrary, in a few TUs characterized by a high-mountain territory, winter snow is recurrent and it may lead to the building of consistent and long-lasting snowpacks that melt away in spring.

Each TU has a reference rain gauge and a set of individually calibrated rainfall thresholds, therefore the warning system is able to issue independent alert levels for each TU. Further details on the SIGMA warning system and on the study area can be found in Martelloni et al. (2011).

Unfortunately, during the test phase of SIGMA, it was observed that a consistent part of the errors committed by the warning system could be related to snow accumulation and depletion. In case of solid precipitations (i.e. snow), heated rain gauges automatically provide the system with a measure of the snow water equivalent, which is not distinguished from rainfall. It was observed that this occurrence leads to several false alarms: the thresholds can be overcome without any landslide occurrence, since water actually accumulates in the snowpack and it is not transferred to the soil. On the other side, several missed alarms were observed during snow melting: the released water triggered some landslides during the days with scarce or absent rainfalls (thus threshold were not exceeded).

To overcome these problems, a simple snow accumulation/melting model (SAMM) was developed and integrated within the SIGMA early warning system.

Given:

1. the scale of the analysis (regional scale);

2. the aforementioned characteristics of the adopted warning system (statistical rainfall thresholds developed for a network of rain gauges each pertaining to a territory with a typical areal extension of few hundreds km^2);

3. the limitation of experimental data (only snow thickness, air temperature and rainfall amount are measured and recorded at few discrete points, mainly corresponding with the rain gauge stations);

SAMM is intended to be an operative computational module to adjust the rainfall measurements provided by the rain gauges when snow-related phenomena are present.

2.2 Snow accumulation-melting model (SAMM)

In this model three different terms of mass are identified: the mass accumulated in the snowpack m_s, the input flow mass m_s^{in}, and the output flow mass m_s^{out}. They can be

HESSD
9, 9391–9423, 2012

expressed by the following equations:

$$\begin{cases} m_s = \rho_s \cdot A \cdot H_s \\ m_s^{in} = \rho_{so} \cdot A \cdot H^{in} \\ m_s^{out} = \rho_s \cdot A \cdot H^{out} \end{cases} \tag{1}$$

where ρ_s, ρ_{so} are respectively the densities of the snowpack and of the newly fallen snow, A is the considered section and H_s the snow height or snowpack thickness. For the principle of mass conservation, the mass variation in the snowpack $\mathrm{d}m_s/\mathrm{d}t$ is due by the difference between the input mass flow Q^{in} and the output mass flow Q^{out}.

$$\frac{\mathrm{d}m_s}{\mathrm{d}t} = Q^{in} - Q^{out}. \tag{2}$$

Equation (2) can be expressed in terms of discrete time variable t:

$$\rho_s(t_1) \cdot H_s(t_1) - \rho_s(t) \cdot H_s(t) = \rho_{so} \cdot H^{in}(t) - \rho_s \cdot H^{out}(t) \tag{3}$$

where $t_1 = t + 1$.

$H_s(t_1)$ is then given by:

$$H_s(t_1) = \frac{\rho_s(t)}{\rho_s(t_1)} \cdot H_s(t) + \frac{\rho_w}{\rho_s(t_1)} \cdot H_w(t) - \frac{\rho_s(t)}{\rho_s(t_1)} \cdot H^{out}(t) \tag{4}$$

where H^{in} has been expressed as a function of the amount of rain H_w, considering the respective water and snow densities ρ_w and ρ_{s0}:

$$\frac{\rho_w}{\rho_{so}} = \frac{\frac{m}{H_w \cdot A}}{\frac{m}{H^{in} \cdot A}} = \frac{H^{in}}{H_w} \Rightarrow H^{in} = \frac{\rho_w}{\rho_{so}} \cdot H_w \tag{5}$$

In Eq. (4) the average density of the snowpack ρ_s and output term H^{out} are not known. The variation in time of the average snowpack density has been considered using empirical equations (see the accumulation module below). $H^{out}(t)$ has been taken into account using empirical equations for depletion process (see melting module below).

HESSD
9, 9391–9423, 2012

2.2.1 Accumulation module

The discrimination between liquid and solid precipitation is essentially played by the temperature of the air T_a. The density of the new fallen snow ρ_{s0} depends largely on wind and T_a (Pahaut, 1975) (Fig. 3).

Since only T_a data were available, ρ_{s0} was approximated by an exponential equation depending on two empirical parameters ($k_{\rho 0}$ and k_{exp}).

$$\rho_{s0}(t_1) = k_{\rho 0} \cdot \exp\left(k_{exp} \cdot (T_a(t_1) - T_0)\right), \tag{6}$$

where T_0 is a threshold temperature under which the precipitation can be considered solid, and the values of the parameters $k_{\rho 0}$ and k_{exp} are obtained by the model calibration (Sect. 2.3).

Equation (6) provides a good approximation for temperature values higher than −5 °C (Fig. 3): this result is due to the typical temperature values experimentally observed in the study area and represented in the dataset used for the model calibration.

The average density of the snowpack ρ_s is a function of time, and is expressed as a weighted average of the density in the previous time interval and the density of new fallen snow,

$$\rho_s(t_1) = \frac{H_s(t)\left(\rho_s(t) + k_{\rho 1}\frac{H_s(t)}{k_{\rho 2}+H_s(t)}\frac{k_\rho}{k_\rho+\rho_s(t)}\right) + H_w(t_1)\rho_w}{H_s(t) + \frac{H_w(t_1)\rho_w}{\rho_0(t_1)}} \tag{7}$$

where

$$k_{\rho 1}\frac{H_s(t)}{k_{\rho 2}+H_s(t)} \cdot \frac{k_\rho}{k_\rho+\rho_s(t)} \tag{8}$$

represents the term of compression due to snowpack weight. Using the terminology from chemical kinetics, in Eq. (8) the snowpack depth H_s is a limiter (compression is

HESSD
9, 9391–9423, 2012

favoured by large H values due to a greater quantity of matter), while the density acts as an inhibitor of the compression process (since a high density tends to oppose to the process of gravitational compression). In Eq. (8), $k_{\rho 1}$, $k_{\rho 2}$, k_ρ are empirical parameters.

A limiter X and an inhibitor Y are respectively defined in a kinetics process as the ratios r_l and r_i:

$$r_l = \frac{X}{k+X} \quad r_i = \frac{k}{k+Y} \tag{9}$$

They play complementary roles: the process goes at full speed (r_l and $r_i \to 1$) for large values of X and for small values of Y, and slows down towards stability (r_l and $r_i \to 0$) for small X values and large Y values.

A third equation gives the height of the mantle as a function of time, taking into consideration the conservation of mass:

$$H_\mathrm{s}(t_1) = \frac{1}{\rho_\mathrm{s}(t_1)}\left(H_\mathrm{s}(t)\rho_\mathrm{s}(t) + H_\mathrm{w}(t_1)\cdot\rho_\mathrm{w}\right) \tag{10}$$

2.2.2 Melting module

Concerning the melting process, the equation of snowpack density can be expressed as

$$\rho_\mathrm{s}(t_1) = \rho_\mathrm{s}(t) + k_{\rho 1}\frac{H_\mathrm{s}(t)}{k_{\rho 2}+H_\mathrm{s}(t)}\frac{k_\rho}{k_\rho+\rho_\mathrm{s}(t)}\frac{T_\mathrm{a}(t_1)}{k_t+T_\mathrm{a}(t)} \tag{11}$$

Unlike Eq. (7), Eq. (11) is not a weighted average, because there is a net variation of mass due to melting. In this process the temperature acts as a limiting factor, because as a result of the melting process itself, water percolates in the snowpack and causes an additional effect of compression. This process, increasing with temperature, is expressed by the term:

$$\frac{T_\mathrm{a}(t_1)}{k_t+T_\mathrm{a}(t_1)} \tag{12}$$

HESSD
9, 9391–9423, 2012

where k_t is an empirical parameter.

The melting process depends on several factors. In this model we take into consideration the temperature, the rain and the amount of mass. The influence of temperature ΔT^* is introduced as a power term expressed by the difference between air temperature and the threshold T_0:

$$\Delta T^* = (T_a(t) - T_0)^{k1} \tag{13}$$

The rain, if present, contributes to the snow melting. Consequently the term α is introduced as a limiter:

$$\alpha = \frac{H_w(t_1)}{k_w + H_w(t_1)} \tag{14}$$

Finally, to simulate the possible effects of refreezing that increases with density and height of the mantle, the amount of mass (expressed as the product of height H_s and density ρ_s) is considered an inhibitor of the dissolution process and can be expressed as the factor

$$\beta = \frac{k_{s1}}{k_{s1} + H_s(t)\rho_s(t)} \tag{15}$$

The Eq. (13), and α and β factors (Eqs. 14 and 15) are then combined in the final equation, which expresses the amount of thawed mass H_{ww} per unit area:

$$H_{ww}(t_1) = (k_2 \Delta T^* + k_3 \alpha)\beta \tag{16}$$

At each time step, through Eq. (22) the height of the snowpack is updated by subtracting the amount of melted snowpack (H_{ww}):

$$H_s(t_1) = \frac{1}{\rho_s(t_1)}(H_s(t)\rho_s(t) - H_{ww}(t_1)) \tag{17}$$

In the Eqs. (13), (14), (15) and (16), k_1, k_2, k_3, k_w, k_{s1} are empirical parameters.

SAMM was conceived to work at hourly time steps, corresponding to the maximum temporal resolution of data at our disposal.

HESSD
9, 9391–9423, 2012

2.3 Parametric identification of the model

The depth of the snowpack measured by a network of instrumented sensors (Fig. 1) was used to calibrate the model: H_s is determined by the temperature, the rainfall, the variable state ρ_s, and the 13 constants of the model $P = p1, p2, \ldots, p13 \in \Re 13$, whose values are determined by the calibration process.

The functional error $E(P)$ is expressed by:

$$E(P) = \frac{1}{N}\sum_{i=1}^{N} w_i \varepsilon_i^2 = \frac{1}{N}\sum_{i=1}^{N} w_i \left(H_i^{\exp} - H_i^{\mathrm{mod}}(\boldsymbol{x}, P)\right)^2 \tag{18}$$

where $H_i^{\exp}$ and H_i^{mod} represent the experimental and the modelled snowpack height, respectively; N is the number of data; w_i is the weight of error ε_i. An optimization algorithm (Flexible Optimized Simplex) (Nelder and Mead, 1965; Himmelblau, 1972; Marsili-Libelli, 1992) was used to estimate the values of the parameters which minimize the functional error $E(P)$ (Eq. 18). This heuristic search algorithm is based on the definition of a simplex, which can be defined as a n-dimensional polytope with the smallest possible number of vertices $(n+1)$: given the domain of the functional error, in our case the simplex is 13-dimensional (14 vertices). Once defined an initial simplex (by assigning an initial condition to each parameters), the algorithm updates the simplex step by step, replacing the worst point, i.e. the point with the higher functional error.

The simplex flexible is an effective approach with several points of strength: it is effective in finding the absolute minimum as it does not stops when relative minimum points are found; it can manage parameters values with different order of magnitude (problems with "high curvature" and "narrow valleys"); the computations are not time-demanding as the algorithm requires a limited number of functional assessments.

The algorithm stops the research process when all vertices of the simplex have the same functional error (flatness test of simplex).

HESSD

9, 9391–9423, 2012

3 Results and discussion

3.1 Results of calibration and validation

The calibration of the model was performed using the dataset of measures recorded by the Doccia di Fiumalbo rain gauge station during the year 2009. Those data were provided by ARPA ("Agenzia Regionale Prevenzione e Ambiente" – Regional Agency Prevention and Environment).

For comparison, in addition to the aforementioned Flexible Optimized Simplex (Sect. 2.3), another calibration process of SAMM was performed using another methodology: the SIMPSA (Cardoso et al., 1996), which is an optimization model based on the combination of a non-linear simplex and simulated annealing algorithms.

Both optimization algorithms defined similar values of the empirical parameters (Table 1) and only little differences could be noticed in the modelled snowpack evolution (Figs. 4 and 5).

To assess the reliability of the snow model and to identify the best calibration algorithm (and relative model configuration), a validation was carried out over an independent data set recoded by the Febbio station. The quality of these data was poorer than that observed in the calibration dataset: an hourly mean and 10-day moving average with exponential weights was used to reduce noise and to overcome the problem of small periods of missing data (Fig. 6).

The validation statistics are shown in Table 2 and prove that the best configuration of SAMM was obtained using the simplex flexible calibration algorithm. According to Ryan et al. (2008), an error of 8.8 cm (this value corresponds to the mean absolute error observed for SAMM validation) is within the measurement errors of the rain gauges.

An overview of the modelling performances of SAMM is provided in Figs. 7 and 8.

A test of the robustness of the model was performed applying a static and dynamic sensitivity analysis.

HESSD
9, 9391–9423, 2012

In the static analysis the sensitivity function $S(P)$ is evaluated:

$$S(P) = \frac{1}{N} \sum_{t=1}^{N} \left| H_t(\boldsymbol{x}, P) - H_t\left(\boldsymbol{x}, P^{\text{nom}}\right) \right| \tag{19}$$

Where H_t ($\boldsymbol{x}$, P^{nom}) is the nominal trajectory and H_t ($\boldsymbol{x}$, P) represents every trajectory obtained perturbing a parameter. The differences of every temporal step are added on a time interval of length N.

This analysis shows that errors are contained: for instance, Fig. 9 shows that for a wide range of T_0 (threshold temperature) and k_1 values close to their nominal values, the maximum mean error is below 10 cm (corresponding to 10 mm of equivalent rainfall).

The effects of the change of the threshold temperature T_0 are displayed in Fig. 9: the nominal value of 0.3 °C is incremented up to 1.3° and decreased to −1.3 °C. The threshold temperature is the most important factor of SAMM, therefore the model is sensible to this parameter, but it also shows a good robustness: in the accumulation phase, the increase by one degree of T_0 causes negligible errors, while for the melting phase higher errors are observed. Other models, in which the threshold temperature usually has values between −1 and 3 °C, also show that a temperature reduction leads to a higher error (US Army Corps of Engineers, 1956; Wigmosta et al., 1994).

3.2 Integration between SAMM and SIGMA

We simulated an integrated use of SAMM and SIGMA using rainfall, temperature and landslide data of the period 2004–2010. This integration is schematically explained in Fig. 11: SAMM acts like a filter depending on the thresholds temperature T_0.

If $T < T_0$ the snow accumulation module keeps the rainfall (if present) and uses it to simulate the building of a snowpack, while a null precipitation enters the SIGMA warning system.

HESSD
9, 9391–9423, 2012

If $T \geq T_0$ the snow melting module returns to SIGMA the water equivalent of snow melting (if present) and the actual raining quantity (if present).

For obvious reasons, SAMM could be implemented only in the 11 TUs equipped with a heated pluviometer (the remaining 8 TUs are provided with standard rain gauges since snow is uncommon). The results of this test (Table 3) show a marked improvement of the landslide forecasting effectiveness within 3 TUs. In the remaining 8 TUs, SIGMA outputs are scarcely influenced by the correction provided by SAMM, because no consistent snowfalls were registered in correspondence of their reference rain gauges during the test period. However, in all TUs, SAMM operates a redistribution of water (coming from rainfall or from snowmelt) that positively influences the outputs of SIGMA in terms of false alarms: the delayed water release allows to better constrain the actual infiltration of water into the ground and thus false alarms can be reduced. Even if false alarms issued at the ordinary criticality level were increased by 5 %, moderate criticality level and high criticality level false alarms were reduced by 20 % and 25 %, respectively.

4 Conclusions

We developed a snow accumulation/melting model (SAMM) aimed at improving (in case of snowmelts and snowfalls) the performances of a regional scale landslide warning system based on statistical rainfall thresholds.

SAMM follows an intermediate approach between physically based and empirical temperature index models. It is based on two modules modelling the snow accumulation and the snowmelt processes. Each module is composed by two equations: a conservation of mass equation models the snowpack thickness and an empirical equation takes into account the snow density. The case study is affected by a relevant scarcity of data: only air temperature and rainfall recordings could be used in future real-time applications. To solve the equations of the model, 13 empirical parameters were introduced. Their optimum value was estimated by means of a calibration procedure in

HESSD
9, 9391–9423, 2012

which the simplex flexible optimization algorithm (Nelder and Mead, 1965; Himmelblau, 1972; Marsili-Libelli, 1992) was used to assess the configuration that minimizes the difference between experimental data of snowpack thickness and model outputs. Validation, which was carried out over an independent dataset, highlighted that the mean error of the model is contained within the rain gauge instrumental error. To a closer insight, however, in some portions of the validation timeline, the modelled snowpack thickness is affected by underestimation or overestimation that can reach 30 cm. Those mismatches are probably heavily conditioned by the necessity of using only rainfall and temperature as input parameters, without explicitly considering other very important physical factors such as solar radiation, wind, atmospheric pressure, air humidity and so on.

The simple formulation of SAMM is conceived to be integrated with empirical landslide forecasting procedures: a threshold temperature (the most important among the aforementioned 13 empirical parameters) switches between the snow accumulation and the snow melting module and adjusts the value of the rainfall amount measured by the rain gauges accordingly. Experimental simulations showed that SAMM could be fruitfully integrated into the Emilia Romagna regional early warning system: the use of SAMM during the period 2004–2010 would have allowed forecasting 54 landslides triggered by snow melting that were not detected by the conventional warning system. The use of SAMM is particularly successful in the mountainous TUs, where solid precipitation is more recurrent, while in the hilly TUs where snow is an exceptional phenomenon (and oftentimes is mixed with rain) the use of SAMM provides limited benefits.

However, the integrated SAMM-SIGMA system presents some advantages: the extreme simplicity and rapidity of the forecasting procedure; the limited number of input data required for calibration and for the operational use (temperature and precipitation); the possibility of exporting the procedure wherever a sufficiently organized meteorological network is present (after a site-specific calibration); the immediate interpretation of the final output, which can be directly put in correspondence with the criticality levels adopted by the Civil Protection Authority.

HESSD
9, 9391–9423, 2012

Acknowledgement. This research has been financed by the Civil Protection Agency of the Emilia Romagna region. The authors would like to thank in particular Angela Gallucci, Sabrina Primerano, Antonio Monni and Demetrio Egidi. ARPA Emilia-Romagna (Regional Agency for Environmental Protection in the Emilia-Romagna region), is fully acknowledged for having provided part of the data used in this work.

References

Aleotti, P.: A warning system for rainfall-induced shallow failures, Eng. Geol., 73, 247–265, 2004.

Bartelt, P. and Lehning, M.: A physical SNOWPACK model for the Swiss avalanche warning: Part I: numerical model, Cold Reg. Sci.Technol., 35, 123–145, 2002.

Baum, R. L., Godt J. W., and Savage, W. Z.: Estimating the timing and location of shallow rainfall induced landslides using a model for transient, unsaturated infiltration, J. Geophys. Res., 115, F03013, doi:10.1029/2009JF001321, 2010.

Bernier, N. B., Bélair, S., Bilodeau, B., and Tong, L.: Near-Surface and Land Surface Forecast System of the Vancouver 2010 Winter Olympic and Paralympic Games, J. Hydrometeorol., 12, 508–530, 2011.

Bloschl, G., Kirnbauer, R., and Gutknecht, D.: Distributed snowmelt simulations in an alpine catchment 1. Model evaluation on the basis of snow cover patterns, Water Resour. Res., 27, 3171–3179, 1991.

Brun, E., Martin, E., Simon, V., Gendre, C., and Coleou, C.: An energy and mass balance model of snowcover suitable for operational avalanche forecasting, J. Glaciol., 35, 333–342, 1989.

Cannon, S. H., Boldt, E. M., Laber, J. L., Kean, J. W., and Staley, D. M.: Rainfall intensity-duration thresholds for postfire debris-flow emergency-response planning, Nat. Hazards, 59, 209–236, 2011.

Cardinali, M., Ardizzone, F., Galli, M., Guzzetti, F., and Reichenbach, P.: Landslide triggered by rapid snow melting: the December 1996–January 1997 event in Central Italy, in: Proceedings European Geophysical Society 1° Plinius Conference on Mediterranean Storms, Maratea, Italy, 14–16 October 1999, 439–448, 2000.

Cardoso, M. E., Salcedo, R. L., and de Azevedo, S. E.: The simplex-simulated annealing approach to continuous non-linear optimization, Comput. Chem. Eng., 20, 1065–1080, 1996.

HESSD

9, 9391–9423, 2012

Snow Accumulation-Melting Model (SAMM)

G. Martelloni et al.

Ceaglio, E., Meusburger, K., Freppaz, M., Zanini, E., and Alewell, C.: Estimation of soil redistribution rates due to snow cover related processes in a mountainous area (Valle d'Aosta, NW Italy), Hydrol. Earth Syst. Sci., 16, 517–528, doi:10.5194/hess-16-517-2012, 2012.

Chleborad, A. F.: Temperature, snowmelt, and the onset of spring season landslides in the central Rocky Mountains, US Geological Survey, Open-File Report 97–27, 35 pp., 1997.

Damiano, E., Olivares, L., and Picarelli, L.: Steep-slope monitoring in unsaturated pyroclastic soils, Eng. Geol., 137–138, 1–12, 2012.

Garen, D. C. and Danny Marks, D.: Spatially distributed energy balance snowmelt modelling in a mountainous river basin: estimation of meteorological inputs and verification of model results, J. Hydrol., 315, 126–153, 2005.

Gokceoglu, C., Sonmez, H., Nefeslioglu, H. A., Duman, T. Y., and Can, T.: Kuzulu landslide (Sivas, Turkey) and landslide-susceptibility map of its near vicinity, Eng. Geol., 81, 65–83, 2005.

Guzzetti, F.: Landslide fatalities and the evaluation of landslide risk in Italy, Eng. Geol., 58, 89–107, 2000.

Guzzetti, F., Reichenbach, P., Cardinali, M., Ardizzone, F., and Galli, M.: The impact of landslides in the Umbria region, central Italy, Nat. Hazards Earth Syst. Sci., 3, 469–486, doi:10.5194/nhess-3-469-2003, 2003.

Himmelblau, D. M.: Applied Non-Linear Programming, McGraw- Hill, New York, 1972.

Herrero, J., Polo, M. J., Moñino, A., and Losada, M. A.: An energy balance snowmelt model in a Mediterranean site, J. Hydrol., 371, 98–107, 2009.

Hock, R.: A distributed temperature-index ice- and snowmelt model including potential direct solar radiation, J. Glaciol., 45, 101–111, 1999.

Hock, R.: Temperature index melt modelling in mountain areas, J. Hydrol., 282, 104–115, 2003.

Jost, G., Moore, R. D., Smith, R., and Gluns, D. R.: Distributed temperature-index snowmelt modelling for forested catchments, J. Hydrol., 420–421, 87–101, 2012.

Kawagoe, S., Kazama, S., and Sarukkalige, P. R.: Assessment of snowmelt triggered landslide hazard and risk in Japan, Cold Reg. Sci. Technol., 58, 120–129, 2009.

Keefer, D. K., Wilson, R. C., Mark, R. K., Brabb, E. E., Brown, W.M.-III, Ellen, S. D., Harp, E. L., Wieczorek, G. F., Alger, C. S., and Zatkin, R. S.: Real-time landslide warning during heavy rainfall, Science, 238, 921–925, 1987.

Kustas, W. P., Rango, A., and Uijlenhoet, R.: A simple energy budget algorithm for the snowmelt runoff model, Water Resour. Res., 30, 1515–1527, 1994.

Li, H.-Y. and Wang, J.: Simulation of snow distribution and melt under cloudy conditions in an Alpine watershed, Hydrol. Earth Syst. Sci., 15, 2195–2203, doi:10.5194/hess-15-2195-2011, 2011.

Marks, D., Domingo, J., Susong, D., Link, T., and Garen, D.: A spazially distributed energy balance snowmelt model for application in mountain basins, Hydrol. Process., 1, 1935–1959, 1999.

Marsili-Libelli, S.: Parameter estimation of ecological models, Ecol. Model., 62, 233–258, 1992.

Martelloni, G., Segoni, S., Fanti, R., and Catani F.: Rainfall thresholds for the forecasting of landslide occurrence at regional scale, Landslides, online first, doi:10.1007/s10346-011-0308-2, 2011.

Martin, E., Timbal, B., and Brun, E.: Downscaling of general circulation model outputs: simulation of the snow climatology of the French Alps and sensitivity to climate change, Clim. Dynam., 13, 45–56, 1996.

Naudet, V., Lazzari, M., Perrone, A., Loperte, A., Piscitelli, S., and Lapenna, V.: Integrated geophysical and geomorphological approach to investigate the snowmelt-triggered landslide of Bosco Piccolo village (Basilicata, southern Italy), Eng. Geol., 98, 156–167, 2008.

Nelder, J. A. and Mead, R.: A simplex method for function minimization, The Computer Journal, 7, 308–313, 1965.

Pahaut, E.: Les cristaux de neige et leurs metamorphoses, Monographie de la meterologie nationale, 96, 61 pp., 1975.

Rango, A. and Martinec, J.: Revisiting the degree-day method for snowmelt computations, Water Resour. Bull., 31, 657–669, 1995.

Ryan, W. A., Doesken, N. J., and Fassnacht, S. R.: Preliminary results of ultrasonic snow depth sensor testing for National Weather Service (NWS) snow measurements in the US, Hydrol. Process., 22, 2748–2757, 2008.

Rosi, A., Segoni, S., Catani, F., and Casagli, N.: Statistical and environmental analyses for the definition of a regional rainfall thresholds system for landslide triggering in Tuscany (Italy), J. Geogr. Sci., 22, 617–629, 2012.

Rousselot, M., Durand, Y., Giraud, G., Merindol, L., and Daniel, L.: Analysis and forecast of extreme new-snow avalanches: a numerical study of the avalanche cycles of February 1999 in France, J. Glaciol., 56, 758–770, 2010.

Segoni, S., Leoni, L., Benedetti, A. I., Catani, F., Righini, G., Falorni, G., Gabellani, S., Rudari, R., Silvestro, F., and Rebora, N.: Towards a definition of a real-time forecasting network for rainfall induced shallow landslides, Nat. Hazards Earth Syst. Sci., 9, 2119–2133, doi:10.5194/nhess-9-2119-2009, 2009.

Segoni, S., Rossi, G., Rosi, A., Catani, F.: Landslides triggered by rainfall: an automated procedure to define consistent intensity-duration thresholds, Environ. Modell. Softw., under review, 2012.

Takeuchi, Y., Torita, H., Nishimura, K., and Hirashima, H.: Study of a large-scale dry slab avalanche and the extent of damage to a cedar forest in the Makunosawa valley, Myoko, Japanm, Ann. Glaciol., 52, 119–128, 2011.

US Army Corps of Engineers: Snow hydrology, summary report of the snow investigations, Technical report, US Army Corps of Engineers, North Pacific Division, Portland, Oregon, 1956.

Wieczorek, G. F.: Landslide triggering mechanisms, in: Landslides: Investigation and Mitigation, edited by: Turner, A. K. and Schuster, R. L., Washington DC, Transportation Research Board, National Research Council, Special Report, 76–90, 1996.

Wigmosta, M. S., Vail, L. W., and Lettenmaier, D. P.: A distributed hydrology-vegetation model for complex terrain, Water Resour. Res., 30, 1665–1679, 1994.

Zanotti, F., Endrizzi, S., Bertoldi, G., and Rigon, R.: The GEOTOP snow module, Hydrol. Process., 18, 3667–3679, doi:10.1002/hyp.5794, 2004.

HESSD
9, 9391–9423, 2012

Table 1. The optimal configuration of SAMM obtained with two different parametric identification techniques.

Parameters	Optimum value (Simplex)	Optimum value (SIMPSA)
k_1	3.25031	3.3993
k_2	0.000926091	0.0010
k_3	15.8715	15.8889
$k_{\rho 1}$	0.432043	0.4372
$k_{\rho 2}$	1.40015	1.4492
k_ρ	0.30003	0.3267
k_t	0.110011	0.1101
k_w	0.0400043	0.0382
k_{s1}	200.02	200.3407
$k_{\rho 0}$	165.016	180
$k_{\exp}$	0.0490052	0.0489
$k_{\rho m}$	94.011	160.0369
T_0	0.300036	0.2757

HESSD
9, 9391–9423, 2012

Table 2. Mean snow depth and errors (measured height – modelled height) for the validation dataset.

	Experimental data	SIMPLEX calibration	SIMPSA calibration
Mean snow depth	41.2 cm	44.9 cm	32.9 cm
Mean absolute error (experimental-model)	–	8.8 cm	10.4 cm

HESSD
9, 9391–9423, 2012

HESSD
9, 9391–9423, 2012

Snow Accumulation-Melting Model (SAMM)

G. Martelloni et al.

Table 3. Results of the simulation of an integrated use of SAMM and SIGMA (period 2004–2010).

Territorial Unit	Landslides identified (SIGMA)	Landslides identified (SAMM + SIGMA)	Improvement (number of landslides)
9	101	105	+4
12	84	112	+28
15	83	105	+22

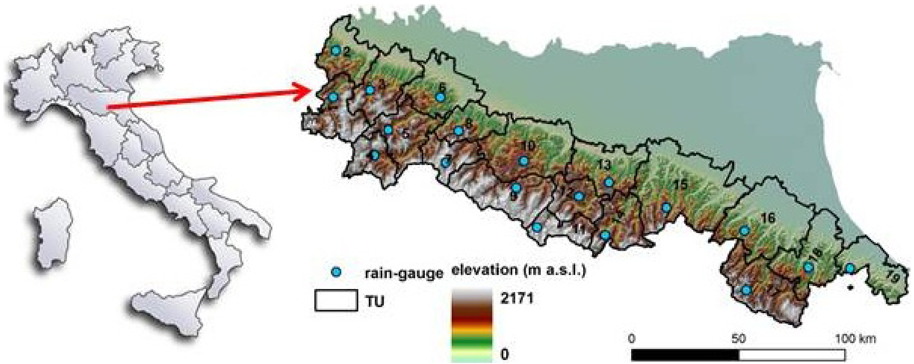

Fig. 1. The Emilia Romagna region. The study area is partitioned into 19 Territorial Units, each provided with a reference rain gauge.

HESSD
9, 9391–9423, 2012

Snow Accumulation-Melting Model (SAMM)

G. Martelloni et al.

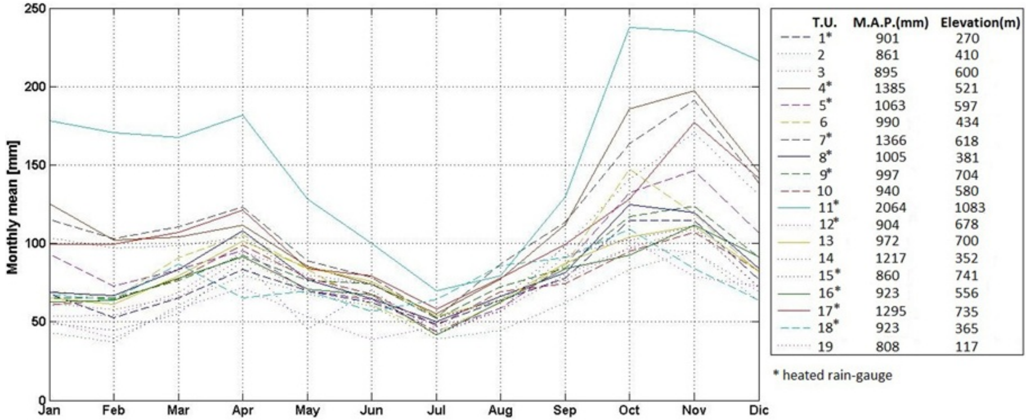

Fig. 2. Pluviometric regime of the 19 territorial units of the Emilia Romagna region.

HESSD
9, 9391–9423, 2012

Snow Accumulation-Melting Model (SAMM)

G. Martelloni et al.

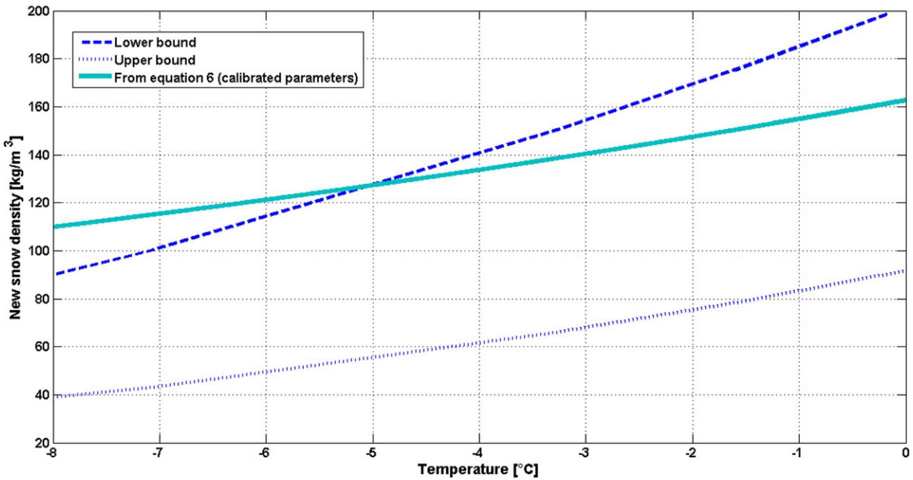

Fig. 3. Comparison between new snow density (obtained by parametric calibration of equation 6) and the typical range of values observed by Pahaut (1975).

HESSD
9, 9391–9423, 2012

Snow Accumulation-Melting Model (SAMM)

G. Martelloni et al.

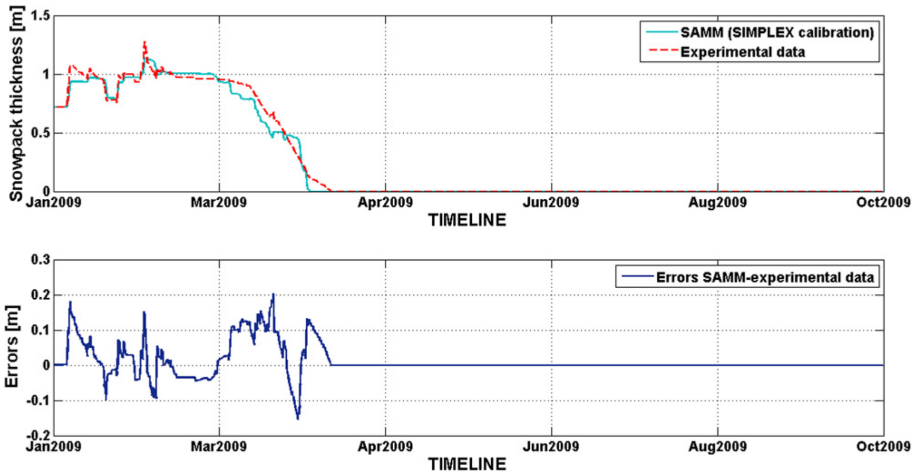

Fig. 4. Calibration of the model with the event January 2009–March 2009 registered by the Doccia di Fiumalbo station, using Simplex flexible algorithm.

HESSD

9, 9391–9423, 2012

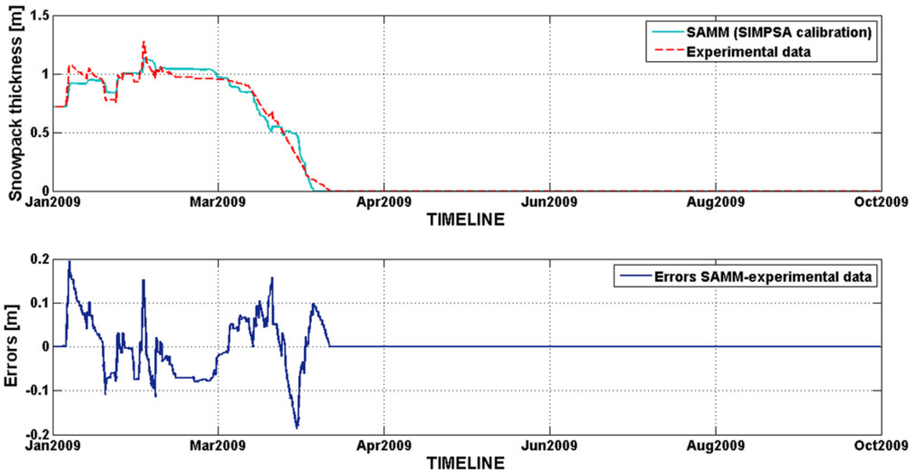

Fig. 5. Calibration of the model with the event January 2009–March 2009 registered by the Doccia di Fiumalbo station, using SIMPSA.

HESSD

9, 9391–9423, 2012

Snow Accumulation-Melting Model (SAMM)

G. Martelloni et al.

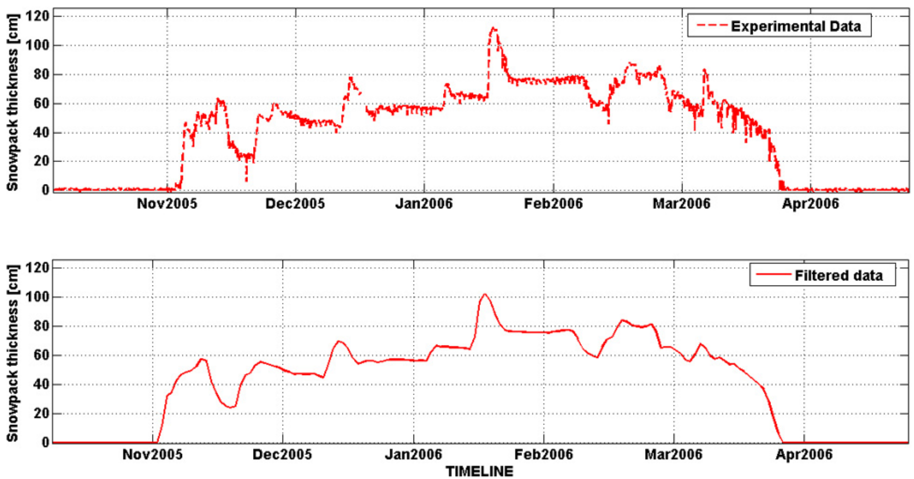

Fig. 6. Example of validation dataset: the experimental data, affected by sensor errors (above), are filtered with a moving average to clear out the noise and to estimate missing data.

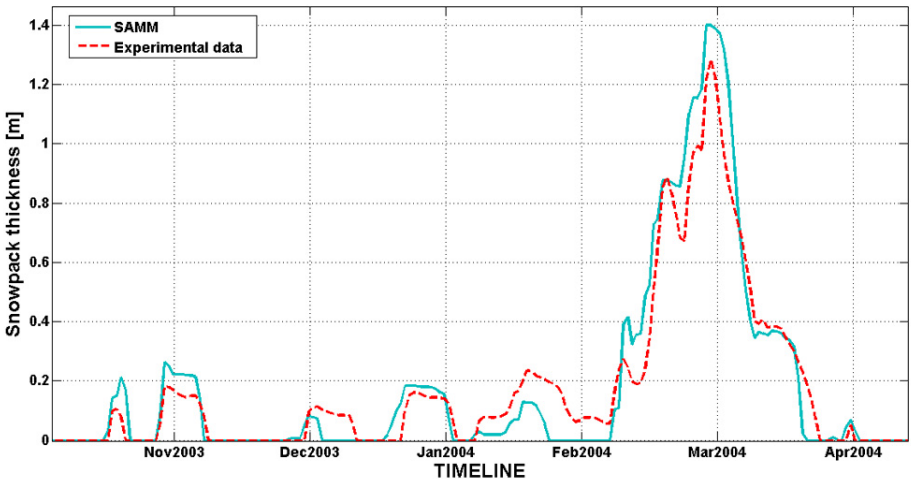

Fig. 7. Validation test of SAMM (Simplex calibration) with the event December 2003–April 2004 registered by Febbio station.

HESSD
9, 9391–9423, 2012

Snow Accumulation-Melting Model (SAMM)

G. Martelloni et al.

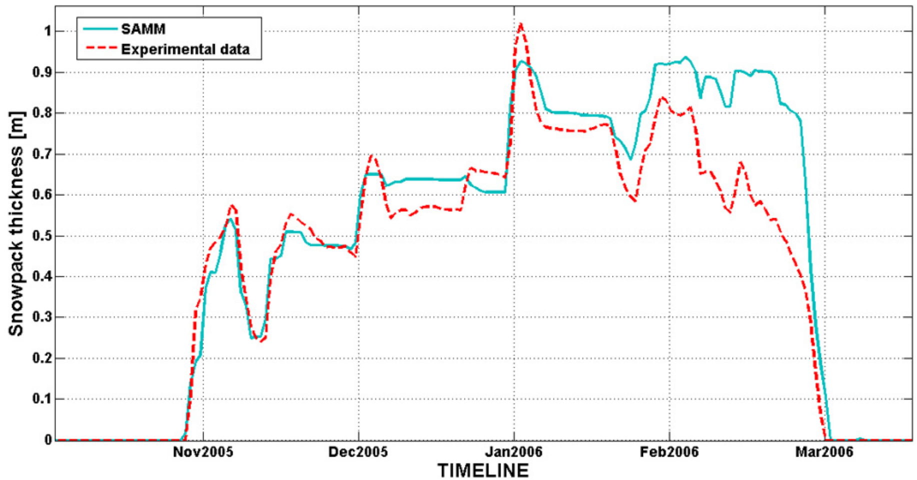

Fig. 8. Validation test of the SAMM (simplex calibration) with the event November 2005–March‘2006 registered by Febbio station.

HESSD
9, 9391–9423, 2012

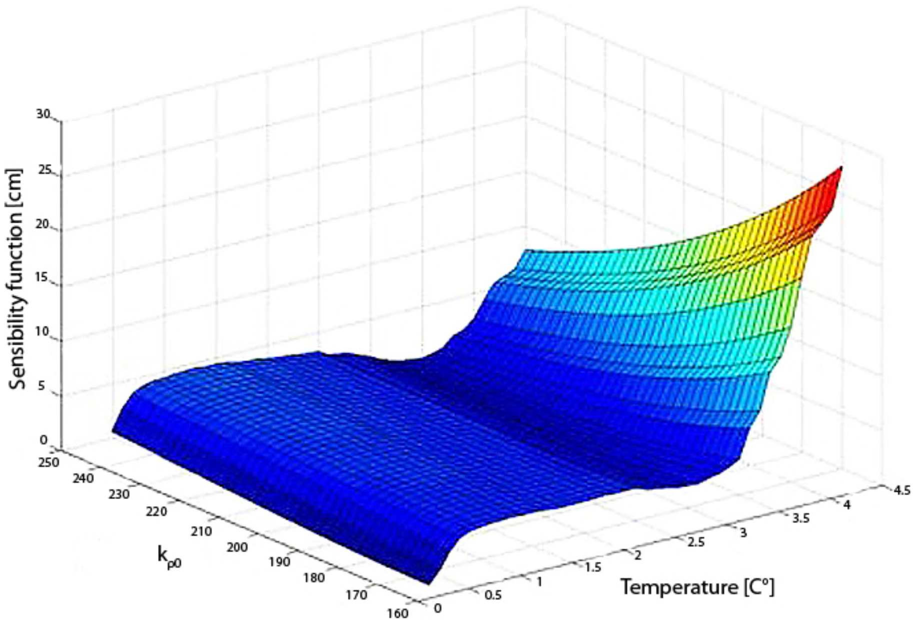

Fig. 9. Static sensitivity analysis of the model for the parameters T_0 (threshold temperature) and $k_{\rho 0}$.

HESSD
9, 9391–9423, 2012

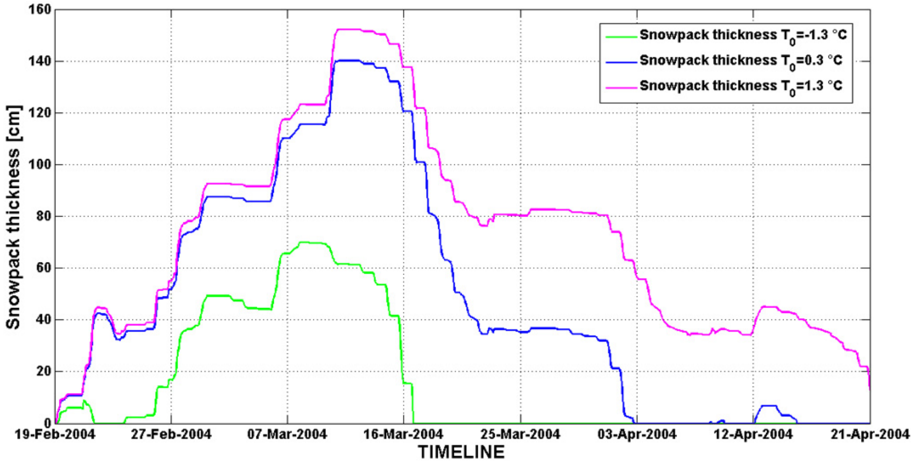

Fig. 10. Dynamic sensitivity analysis of the model for three different values of threshold temperature.

HESSD
9, 9391–9423, 2012

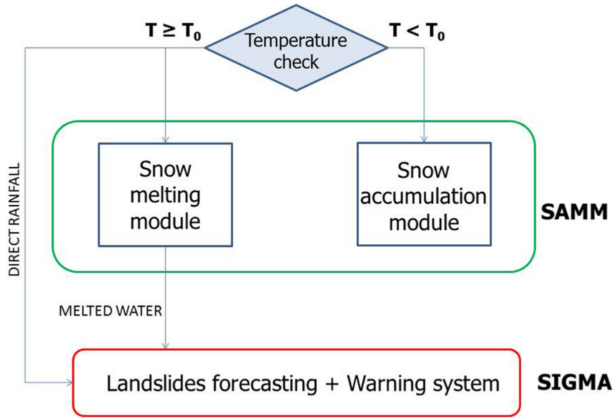

Fig. 11. Integrated system SAMM-SIGMA for landslides forecasting.

HESSD
9, 9391–9423, 2012